
CHAPTER 36

MATERIAL DAMPING AND SLIP DAMPING

L. E. Goodman

INTRODUCTION

The term *damping* as used in this chapter refers to the energy-dissipation properties of a material or system under cyclic stress, but excludes energy-transfer devices such as dynamic absorbers. With this understanding of the meaning of the word, energy must be dissipated within the vibrating system. In most cases a conversion of mechanical energy to heat occurs. For convenience, damping is classified here as (1) material damping and (2) system damping. Material properties and the principles underlying the measurement and prediction of damping magnitude are discussed in this chapter. For application to specific engineering problems, see Chap. 37.

MATERIAL DAMPING

Without a source of external energy, no real mechanical system maintains an undiminished amplitude of vibration. *Material damping* is a name for the complex physical effects that convert kinetic and strain energy in a vibrating mechanical system consisting of a volume of macrocontinuous (solid) matter into heat. Studies of material damping are employed in solid-state physics as guides to the internal structure of solids. The damping capacity of materials is also a significant property in the design of structures and mechanical devices; for example, in problems involving mechanical resonance and fatigue, shaft whirl, instrument hysteresis, and heating under cyclic stress. Three types of material that have been studied in detail are:

1. *Viscoelastic materials.*¹ The idealized linear behavior generally assumed for this class of materials is amenable to the laws of superposition and other conventional rheological treatments including model analog analysis. In most cases linear (Newtonian) viscosity is considered to be the principal form of energy dissipation. Many polymeric materials, as well as some other types of materials, may be treated under this heading.
2. *Structural metals and nonmetals.*² The linear dissipation functions generally assumed for the analysis of viscoelastic materials are not, as a rule, appropriate

for structural materials. Significant nonlinearity characterizes structural materials, particularly at high levels of stress. A further complication arises from the fact that the stress and temperature histories may affect the material damping properties markedly; therefore, the concept of a stable material assumed in viscoelastic treatments may not be realistic for structural materials.

3. *Surface coatings.* The application of coatings to flat and curved surfaces to enhance energy dissipation by increasing the losses associated with fluid flow is a common device in acoustic noise control. These coatings also take advantage of material and interface damping through their bond with a structural material. They are treated in detail in Chap. 37.

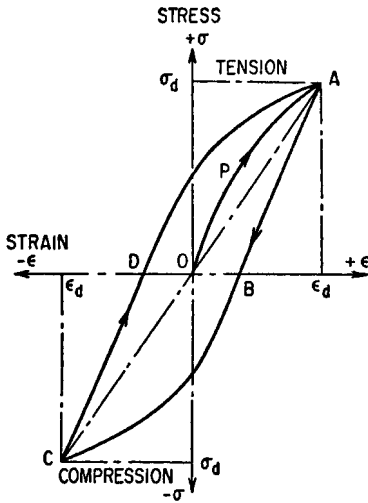


FIGURE 36.1 Typical stress-strain (or load-deflection) hysteresis loop for a material under cyclic stress.

Material damping of macrocontinuous media may be associated with such mechanisms as plastic slip or flow, magnetomechanical effects, dislocation movements, and inhomogeneous strain in fibrous materials. Under cyclic stress or strain these mechanisms lead to the formation of a stress-strain hysteresis loop of the type shown in Fig. 36.1. Since a variety of inelastic and anelastic mechanisms can be operative during cyclic stress, the unloading branch *AB* of the stress-strain curve falls below the initial loading branch *OPA*. Curves *OPA* and *AB* coincide only for a perfectly elastic material; such a material is never encountered in actual practice, even at very low stresses. The damping energy dissipated per unit volume during one stress cycle (between stress limits $\pm\sigma_d$ or strain limits $\pm\epsilon_d$) is equal to the area within the hysteresis loop *ABCDA*.

SLIP DAMPING

In contrast to material damping, which occurs within a volume of solid material, slip damping³ arises from boundary shear effects at mating surfaces, or joints between distinguishable parts. Energy dissipation during cyclic shear strain at an interface may occur as a result of dry sliding (Coulomb friction), lubricated sliding (viscous forces), or cyclic strain in a separating adhesive (damping in a viscoelastic layer between mating surfaces).

SIGNIFICANCE OF MECHANICAL DAMPING AS AN ENGINEERING PROPERTY

Large damping in a structural material may be either desirable or undesirable, depending on the engineering application at hand. For example, damping is a desirable property to the designer concerned with limiting the peak stresses and extending the fatigue life of structural elements and machine parts subjected to

near-resonant cyclic forces or to suddenly applied forces. It is a desirable property if noise reduction is of importance. On the other hand, damping is undesirable if internal heating is to be avoided. It also can be a source of dynamic instability of rotating shafts and of error in sensitive instruments.

Resonant vibrations of large amplitude are encountered in a variety of modern devices, frequently causing rough and noisy operation and, in extreme cases, leading to seriously high repeated stresses. Various types of damping may be employed to minimize these resonant vibration amplitudes. Although special damping devices of the types described in Chap. 6 may be used to transfer energy from the system, there are many situations in which auxiliary dampers are not practical. Then accurate estimation of material and slip damping becomes important.

When an engineering structure is subjected to a harmonic exciting force $F_g \sin \omega t$, an induced force $F_d \sin (\omega t - \phi)$ appears at the support. The ratio of the amplitudes, F_d/F_g , is a function of the exciting frequency ω . It is known as the vibration amplification factor. At resonance, when $\phi = 90^\circ$, this ratio becomes the resonance amplification factor⁴ A_r :

$$A_r = \frac{F_d}{F_g} \tag{36.1}$$

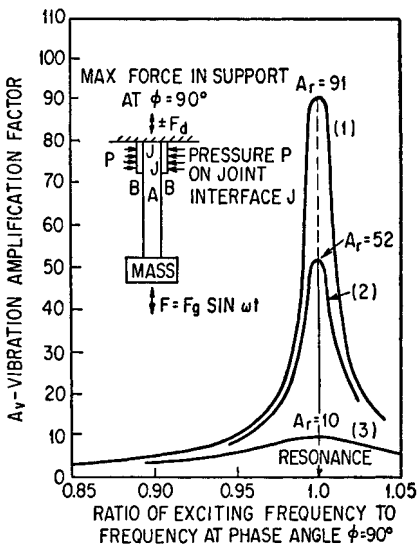


FIGURE 36.2 Effect of material and slip damping on vibration amplification. Curve (1) illustrates case of small material and slip damping; (2) one damping is large while other is small; (3) both material and slip damping are large.

This condition is pictured schematically in Fig. 36.2 for low, intermediate, and high damping (curves 1, 2, 3, respectively).

The magnitude of the resonance amplification factor varies over a wide range in engineering practice.⁵ In laboratory tests, values as large as 1000 have been observed. In actual engineering parts under high stress, a range of 500 to 10 is reasonably inclusive. These limits are exemplified by an airplane propeller, cyclically stressed in the fatigue range, which displayed a resonance amplification factor of 490, and a double leaf spring with optimum interface slip damping which was observed to have a resonance amplification factor of 10. Because of the wide range of possible values of A_r , each case must be considered individually.

METHODS FOR MEASURING DAMPING PROPERTIES

STRESS-STRAIN (OR LOAD-DEFLECTION) HYSTERESIS LOOP

The hysteresis loop illustrated in Fig. 36.1 provides a direct and easily interpreted measure of damping energy. To determine damping at low stress levels requires

instruments of extreme sensitivity. For example, the width (DB in Fig. 36.1) of the loop of chrome steel at an alternating direct-stress level of 103 MPa^* is less than 2×10^{-6} . High-sensitivity and high-speed transducers and recording devices are required to attain sufficient accuracy for the measurement of such strains. For metals in general, extremely long gage lengths are required to measure damping in direct stress by the hysteresis loop method if the peak stress is less than about 60 percent of the fatigue limit. Under torsional stress, however, greater sensitivity is possible and the hysteresis loop method is applicable to low stress work.

PROCEDURES EMPLOYING A VIBRATING SPECIMEN

The following methods of measuring damping utilize a vibrating system in which the deflected member, usually acting as a spring, serves as the specimen under test. For example, one end of the specimen may be fixed and the other end attached to a mass which is caused to vibrate; alternatively, a freely supported beam or a tuning fork may be used as the specimen vibrating system.⁶ In any arrangement the damping is computed from the observed vibratory characteristics of the system.

In one class of these procedures the rate of decay of free damped vibration is measured. Typical vibration decay curves are shown in Fig. 36.3. The measure of damping usually used, the *logarithmic decrement*, is the natural logarithm of the ratio of any two successive amplitudes [see Eq. (2.19)]:

$$\Delta = \ln \frac{x_n}{x_{n+1}} \approx \frac{\Delta x}{x_n} \quad (36.2)$$

The relation between logarithmic decrement and other units used to measure damping is given in Eq. (36.16). Vibration decay tests can be performed under a variety of stress and temperature conditions, and may utilize many different procedures for releasing the specimen and recording the vibration decay. It is essential to minimize the loss of energy either to the specimen supports or in acoustic radiation.

A second class of vibrating specimen procedures makes use of the fact, illustrated in Fig. 36.2, that higher damping is associated with a broader peak in the frequency response or resonance curve. If the exciting force is held constant and the exciting frequency varied, measurement of the steady-state amplitude of motion (or stress) yields a curve similar to those shown in Fig. 36.2. The damping is then determined by measuring the width of the curve at an amplification factor equal to

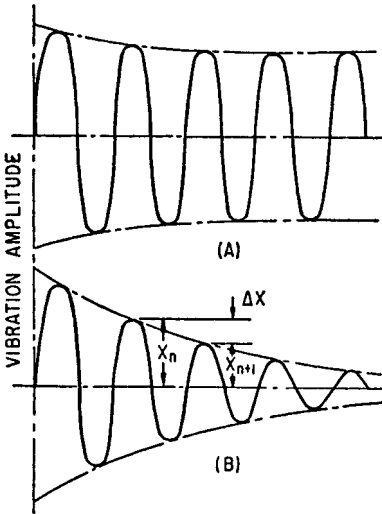


FIGURE 36.3 Typical vibration decay curves: (A) low decay rate, small damping, and (B) high decay rate, large damping.

* $1 \text{ MPa} = 10^6 \text{ N/m}^2 = 146.5 \text{ lb/in.}^2$ ($103 \text{ MPa} = 15,000 \text{ lb/in.}^2$).

0.707 A_r . If a horizontal line drawn at this ordinate intercepts the resonance curve at frequency ratios f_1/f_n and f_2/f_n ,

$$\Delta = \pi \left(\frac{f_2}{f_n} - \frac{f_1}{f_n} \right) \tag{36.3}$$

The quantity $(f_2 - f_1)$ is the *bandwidth at the half-power point*. This procedure has the advantage of requiring only steady-state tests. As in the case of the free-decay procedure, only the relative amplitude of the response need be measured. However, the procedure does impose a particular stress history. If the system behavior should be markedly nonlinear, the shape of the resonance curve will not be that assumed in the derivation of Eq. (36.3).

If a system is operated exactly at resonance, the resonance amplification factor A_r is the ratio of the (induced) force F_d to the exciting force F_g [see Eq. (36.1)]. In direct application of this equation, F_g is usually made controllable and F_d computed from strain or displacement measurements. The principle has been applied to the measurement of damping in a large structure⁷ and in simple test specimens. It can take account of high stress magnitude and of stress history as controlled variables. The natural frequency of vibration of a specimen can be altered so that damping as a function of frequency may be studied, but it is usually difficult to make such measurements over a wide frequency range. This technique requires accurately calibrated apparatus since measurements are absolute and not relative.

LATERAL DEFLECTION OF ROTATING CANTILEVER METHOD

The principle of the lateral deflection method is illustrated in Fig. 36.4. If test specimen S is loaded by arm-weight combination A — W , the target T deflects vertically downward from position 1 to position 2. If the arm-specimen combination is rotated by spindle B , as in a rotating cantilever-beam fatigue test, target T moves from posi-

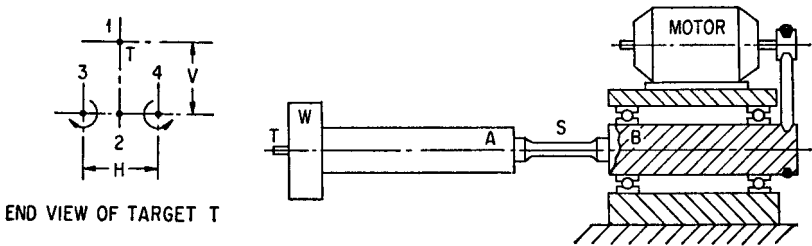


FIGURE 36.4 Principle of rotating cantilever beam method for measuring damping.

tion 2 to position 3 for clockwise rotation. If the direction of rotation is counterclockwise, the target moves from position 3 horizontally to position 4. The horizontal traversal H is a direct measure of the total damping absorbed by the rotating system.⁸

A modification of the lateral deflection method is the *lateral force method*. The end of the rotating beam is confined and the lateral confining force is measured instead of the lateral deflection H . This modification is particularly useful for measurements of low modulus materials, such as plastic and viscoelastic materials.⁹

The advantages of the rotating cantilever beam method are (1) the test variables, stress magnitude, stress history, and frequency, may be easily and independently controlled so that this method is satisfactory for intermediate and high stress levels, and (2) it yields not only data on damping but also fatigue and elasticity properties.

The disadvantages of this method are (1) the tests are rather time-consuming, (2) accuracy is often questionable at low stress levels (below about 20 percent of the fatigue limit) due to the small value of the horizontal traversal H , and (3) the method can be used under rotating-bending conditions only.

HIGH-FREQUENCY PULSE TECHNIQUES

A sequence of elastic pulses generated by a transducer such as a quartz crystal cemented to the front face of a specimen is reflected at the rear face and received again at the transducer. The frequencies are in the megacycle range. The velocity of such waves provides a measure of the elastic constants of the specimen; their decay rates provide a measure of the material damping.¹⁰ This technique has been widely employed in the study of the viscoelastic properties of polymers and the elastic properties of crystals. So far as measurement of damping is concerned, it is open to the objection that the attenuation may be due to scattering by imperfections rather than to internal friction.

FUNDAMENTAL RELATIONSHIPS

Two general types of units are used to specify the damping properties of structural materials: (1) the energy dissipated per cycle in a structural element or test specimen and (2) the ratio of this energy to a reference strain energy or elastic energy. Absolute damping energy units are:

D_0 = *total damping energy* dissipated by entire specimen or structural element per cycle of vibration, N·m/cycle

D_a = *average damping energy*, determined by dividing total damping energy D_0 by volume V_0 of specimen or structural element which is dissipating energy, N·m/m³/cycle

D = *specific damping energy*, work dissipated per unit volume and per cycle at a point in the specimen, N·m/m³/cycle

Of these absolute damping energy units, the total energy D_0 usually is of greatest interest to the engineer. The average damping energy D_a depends upon the shape of the specimen or structural element and upon the nature of the stress distribution in it, even though the specimens are made of the same material and have been subjected to the same stress distribution at the same temperature and frequency. Thus, quoted values of the average damping energy in the technical literature should be viewed with some reserve.

The specific damping energy D is the most fundamental of the three absolute units of damping since it depends only on the material in question and not on the shape, stress distribution, or volume of the vibrating element. However, most of the methods discussed previously for measuring damping properties yield data on total damping energy D_0 rather than on specific damping energy D . Therefore, the development of the relationships between these quantities assumes importance.

RELATIONSHIP BETWEEN D_0 , D_a , AND D

If the specific damping energy is integrated throughout the stressed volume,

$$D_0 = \int_0^{V_0} D \, dV \quad (36.4)$$

This is a triple integral; $dV = dx \, dy \, dz$ and D is regarded as a function of the space coordinates x , y , z . If there is only one nonzero stress component, the specific damping energy D may be considered a function of the stress level σ . Then

$$D_0 = \int_0^{\sigma_d} D \frac{dV}{d\sigma} \, d\sigma \quad (36.5)$$

In this integration, V is the volume of material whose stress level is less than σ . The integration is a single integral, and σ_d is the peak stress. The integrands may be put in dimensionless form by introducing D_d , the specific damping energy associated with the peak stress level reached anywhere in the specimen during the vibration (i.e., the value of D corresponding to $\sigma = \sigma_d$). Then

$$D_0 = D_d V_0 \alpha \quad (36.6)$$

where

$$\alpha = \int_0^1 \left(\frac{D}{D_d} \right) \frac{d(V/V_0)}{d(\sigma/\sigma_d)} \, d \left(\frac{\sigma}{\sigma_d} \right) \quad (36.7)$$

The average damping energy is

$$D_a = \frac{D_0}{V_0} = D_d \alpha \quad (36.8)$$

The relationship between the damping energies D_0 , D_a , and D depends upon the dimensionless damping energy integral α . The integrand of α may be separated into two parts: (1) a damping function D/D_d which is a property of the material and (2) a volume-stress function $d(V/V_0)/d(\sigma/\sigma_d)$ which depends on the shape of the part and the stress distribution.

RELATIONSHIP BETWEEN SPECIFIC DAMPING ENERGY AND STRESS LEVEL

Before the damping function D/D_d can be determined, the specific damping energy D must be related to the stress level σ . Data of this type for typical engineering materials are given in Figs. 36.10 and 36.11. These results illustrate the fact that the damping-stress relationship for all materials cannot be expressed by one simple function. For a large number of structural materials in the low-intermediate stress region (up to 70 percent of σ_e the fatigue strength at 2×10^7 cycles), the following relationship is reasonably satisfactory:

$$D = J \left(\frac{\sigma}{\sigma_e} \right)^n \quad (36.9)$$

Values of the constants J and n are given in Table 36.5 and Fig. 36.10. In general, $n = 2.0$ to 3.0 in the low-intermediate stress region but may be much larger at high stress levels. Where Eq. (36.9) is not applicable, as in the high stress regions of Figs.

36.10 and 36.11 or in the case of the 403 steel alloy of Fig. 36.9, analytical expressions are impractical and a graphical approach is more suitable for the computation of α .

VOLUME-STRESS FUNCTION

The volume-stress function (V/V_0) may be visualized by referring to the dimensionless volume-stress curves shown in Fig. 36.5. The variety of specimen types included in this figure [tension-compression member (1) to turbine blade (9)] is representative of those encountered in practice. These curves give the fraction of the total volume which is stressed below a certain fraction of the peak stress. In a torsion member, for example, 30 percent of the material is at a stress lower than 53 percent of the peak stress. The volume-stress curves for a part having a reasonably uniform stress, i.e., having most of its volume stressed near the maximum stress, are in the region of this diagram labeled *H*. By contrast, curves for parts having a large stress

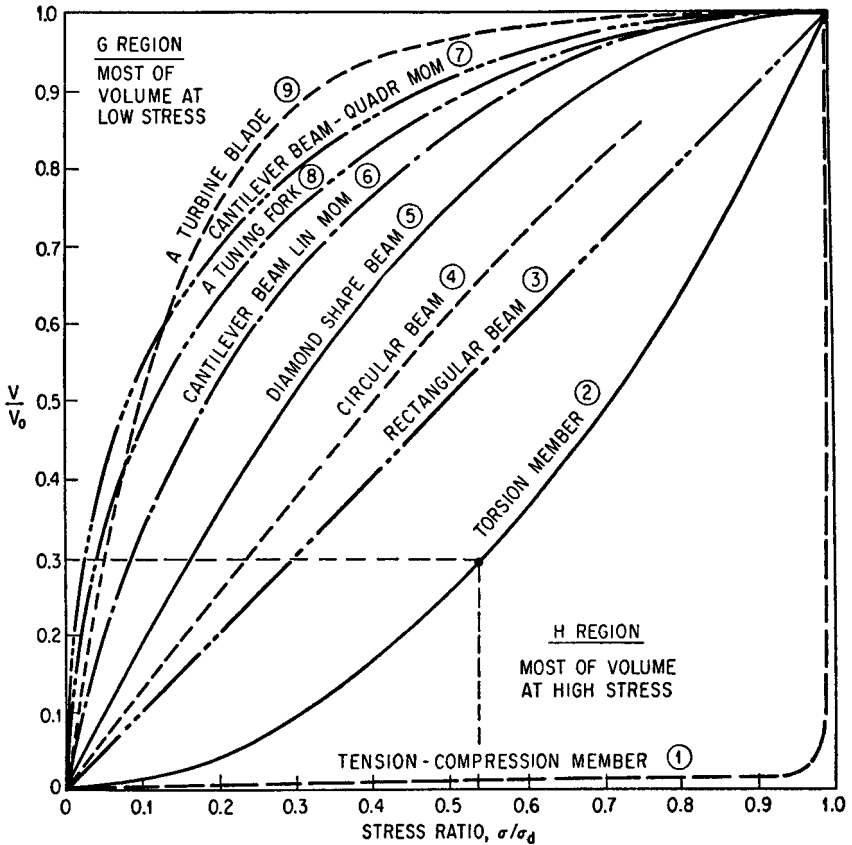


FIGURE 36.5 Volume-stress functions for various types of parts. (See Table 36.1 for additional details on parts.)

gradient (such as a notched beam in which very little volume is at the maximum stress and practically all of the volume is at a very low stress) are in the G region.

In order to illustrate representative values of α for several cases of engineering interest, the results of selected analytical and graphical computations¹¹ are summarized in Table 36.1 and in Fig. 36.6. In Fig. 36.6 the effect of the damping exponent n on the value of α for different types of representative specimens is illustrated. Note the wide range of α encountered for $n = 2.4$ (representative of many materials at low and intermediate stress) and for $n = 8$ (representative of materials at high stress, as shown in the next section).

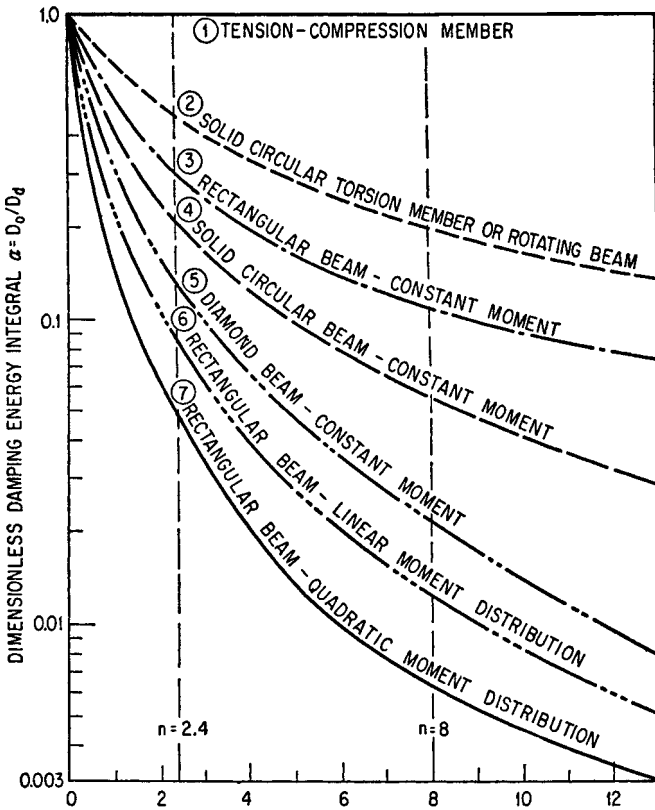


FIGURE 36.6 Damping exponent n in equation $D = J(\sigma/\sigma_c)^n$.

RATIO OF DAMPING ENERGY TO STRAIN ENERGY

Owing to the complexity of the sources of material damping, the use of relative damping energy units does not produce all the advantages that might otherwise be associated with a nondimensional quantity. One motivation for the use of such units, however, is their direct relation to several conventional damping tests. The *logarithm-*

TABLE 36.1 Expressions and Values for α and β/α for Various Stress Distribution and Damping Functions

Type of specimen and loading as designated in Fig. 36.1	Volume-stress function V/V_0	Dimensionless damping energy integral α for various damping functions				Dimensionless strain energy integral β	β/α if $n = 8$	
		General case $D = f(\sigma)$	For special case $D = J(\sigma/\sigma_d)^n$					
			For any value of n	$n = 2.4$	$n = 8$			
1 Tension-compression member		1	1	1	1.0	1		
2 Cylindrical torsion member or rotating beam	$\left(\frac{\sigma}{\sigma_d}\right)^2$	$\left[1 + \frac{\sigma_d}{2D_0} \frac{dD_0}{d\sigma_d}\right]^{-1}$	$\frac{2}{n+2}$	0.45	0.20	0.5	2.5	
3 Rectangular beam under uniform bending	$\frac{\sigma}{\sigma_d}$	$\left[1 + \frac{\sigma_d}{D_0} \frac{dD_0}{d\sigma_d}\right]^{-1}$	$\frac{1}{n+1}$	0.29	0.11	0.33	3.0	
4 Cylindrical beam under uniform bending	$\frac{2}{\pi} \left[\frac{\sigma}{\sigma_d} \sqrt{1 - \left(\frac{\sigma}{\sigma_d}\right)^2} + \sin^{-1}\left(\frac{\sigma}{\sigma_d}\right) \right]$		$\frac{1}{\sqrt{\pi}} \frac{2}{n+2} \frac{\Gamma\left(\frac{n+1}{2}\right)}{\Gamma\left(\frac{n+2}{2}\right)}$	0.21	0.055	0.24	4.5	
5 Diamond beam under uniform bending	$2 \frac{\sigma}{\sigma_d} - \left(\frac{\sigma}{\sigma_d}\right)^2$	$\left[1 + \frac{2\sigma_d}{D_0} \frac{dD_0}{d\sigma_d} + \frac{\sigma_d^2}{2D_0} \frac{d^2D_0}{d\sigma_d^2}\right]^{-1}$	$\frac{2}{n^2 + 3n + 2}$	0.13	0.022	0.17	7.7	
6 Rectangular beam having bending moment shown	$M_x = \frac{x}{L} M_0$	$\frac{\sigma}{\sigma_d} \left[1 - \log_e \frac{\sigma}{\sigma_d}\right]$	$\left[1 + \frac{3\sigma_d}{D_0} \frac{dD_0}{d\sigma_d} + \frac{\sigma_d^2}{D_0} \frac{d^2D_0}{d\sigma_d^2}\right]^{-1}$	$\frac{1}{(n+1)^2}$	0.088	0.012	0.11	9.1
	$M_x = \left(\frac{x}{L}\right)^2 M_0$	$2 \sqrt{\frac{\sigma}{\sigma_d}} - \frac{\sigma}{\sigma_d}$	$\left[1 + \frac{5\sigma_d}{D_0} \frac{dD_0}{d\sigma_d} + \frac{2\sigma_d^2}{D_0} \frac{d^2D_0}{d\sigma_d^2}\right]^{-1}$	$\frac{1}{2n^2 + 3n + 1}$	0.051	0.0065	0.067	10.0
8 Tuning fork in bending	$K \frac{\sigma}{\sigma_d} \left[1 - \log_e \frac{\sigma}{\sigma_d}\right]$	$K \left[1 + \frac{3\sigma_d}{D_0} \frac{dD_0}{d\sigma_d} + \frac{\sigma_d^2}{D_0} \frac{d^2D_0}{d\sigma_d^2}\right]^{-1}$	$\frac{K}{(n+1)^2}$	For $K = 0.8 \rightarrow$	0.091	0.0099	0.089	9.0

Note: $\beta/\alpha = 1$ for all cases if $n = 2$.

mic decrement Δ is defined by Eq. (36.2). Other energy ratio units are tabulated and defined below. In this chapter, the energy ratio unit termed *loss factor* is used as the reference unit.

In defining the various energy ratio units, it is important to distinguish between loss factor η_s of a specimen or part (having a variable stress distribution) and the loss factor η for a material (having a uniform stress distribution). By definition the loss factor of a specimen (identified by subscript s) is

$$\eta_s = \frac{D_0}{2\pi W_0} \tag{36.10}$$

where the total damping D_0 in the specimen is given by Eq. (36.6). The total strain energy in the part is of the form

$$W_0 = \int_0^{V_0} \frac{1}{2} \left(\frac{\sigma^2}{E} \right) dV = \frac{1}{2} \left(\frac{\sigma_d^2}{E} \right) V_0 \beta \tag{36.11}$$

where E denotes a modulus of elasticity and β is a dimensionless integral whose value depends upon the volume-stress function and the stress distribution:

$$\beta = \int_0^1 \left(\frac{\sigma}{\sigma_d} \right)^2 \frac{d(V/V_0)}{d(\sigma/\sigma_d)} d \left(\frac{\sigma}{\sigma_d} \right) \tag{36.12}$$

On substituting Eq. (36.6) and Eq. (36.11) in Eq. (36.10), it follows that

$$\eta_s = \frac{E}{\pi} \frac{D_d}{\sigma_d^2} \frac{\alpha}{\beta} \tag{36.13}$$

If the specimen has a uniform stress distribution, $\alpha = \beta = 1$ and the specimen loss factor η_s becomes the material loss factor η ; in general, however,

$$\eta = \frac{ED_d}{\pi\sigma_d^2} = \eta_s \frac{\beta}{\alpha} \tag{36.14}$$

Other energy ratio (or relative energy) damping units in common use are defined below:

For specimens with variable stress distribution:

$$\eta_s = (\tan \phi)_s = \frac{\Delta_s}{\pi} = \frac{\psi_s}{\pi} = \left(\frac{\delta\omega}{\omega_n} \right)_s = \frac{1}{(A_r)_s} = \frac{1}{Q_s} = \frac{ED_d}{\pi\sigma_d^2} \left(\frac{\alpha}{\beta} \right) \tag{36.15}$$

For materials or specimens with uniform stress distribution:

$$\eta = \tan \phi = \frac{\Delta}{\pi} = \frac{\psi}{\pi} = \frac{\delta\omega}{\omega_n} = \frac{1}{A_r} = \frac{1}{Q} = Q^{-1} = \frac{ED_d}{\pi\sigma_d^2} \tag{36.16}$$

where η = loss factor of material = dissipation factor (high loss factor signifies high damping)

$\tan \phi$ = loss angle, where ϕ is phase angle by which strain lags stress in sinusoidal loading

$\psi = \pi\eta$ = specific damping capacity

$\delta\omega/\omega_n$ = (bandwidth at half-power point)/(natural frequency) [see Eq. (36.3)]

A_r = resonance amplification factor [see Eq. (36.1)]

$Q = 1/\eta =$ measure of the sharpness of a resonance peak and amplification produced by resonance

The material properties are related to the specimen properties as follows:

$$\psi = \psi_s \frac{\beta}{\alpha} \quad \Delta = \Delta_s \frac{\beta}{\alpha} \quad A_r = (A_r)_s \frac{\alpha}{\beta} \quad (36.17)$$

Thus, the various energy ratio units, as conventionally expressed for specimens, depend not only on the basic material properties D and E but also on β/α . The ratio β/α depends on the form of the damping-stress function and the stress distribution in the specimen. As in the case of average damping energy, D_a , the loss factor or the logarithmic decrement for specimens made from exactly the same material and exposed to the same stress range, frequency, temperature, and other test variables may vary significantly if the shape and stress distribution of the specimen are varied. Since data expressed as logarithmic decrement and similar energy ratio units reported in the technical literature have been obtained on a variety of specimen types and stress distributions, any comparison of such data must be considered carefully. The ratio β/α may vary for specimens of exactly the same shape if made from materials having different damping-stress functions. For different specimens made of exactly the same materials, the variation in β/α also may be large, as shown in Fig. 36.7. For example,

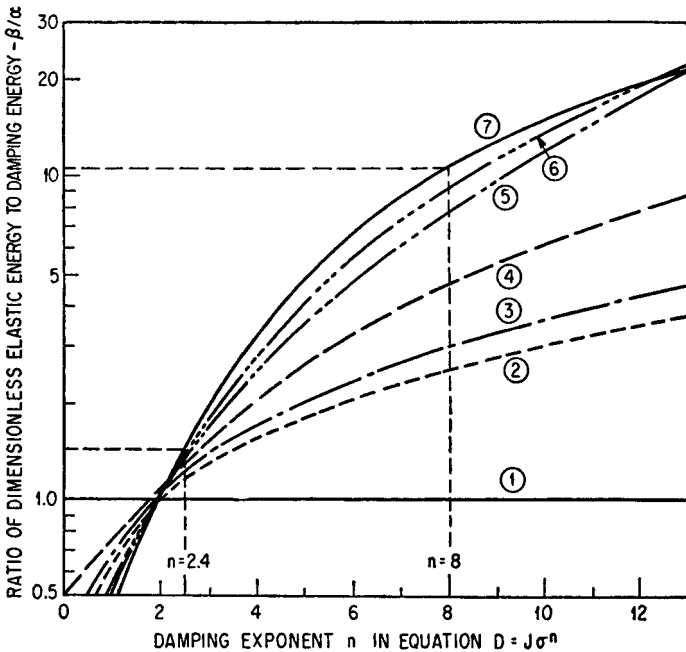


FIGURE 36.7 Effect of damping exponent n on ratio β/α for $D = J\sigma^n$. Curves are (1) tension-compression member; (2) solid circular torsion member or rotating beam; (3) rectangular beam—constant moment; (4) solid circular beam—constant moment; (5) diamond beam—constant moment; (6) rectangular beam—linear moment distribution; and (7) rectangular beam—quadratic moment distribution.

for a material and stress region for which the damping exponent $n = 2.4$ (characteristic of metals at low and intermediate stress), the value of β/α shown in Table 36.1 varies from 1 for a tension-compression member to 1.6 for a rectangular beam with quadratic moment distribution. If $n = 8$ (characteristic of materials at high stress), the variation is from 1 to 10, and larger for beams with a higher stress gradient.

It is possible, for a variety of types of beams, to separate the ratio β/α into two factors: ¹² (1) a cross-sectional shape factor K_c which quantitatively expresses the effect of stress distribution on a cross section, and (2) a longitudinal stress distribution factor K_s , which expresses the effect of stress distribution along the length of the beam. Then

$$\frac{\beta}{\alpha} = K_s K_c \tag{36.18}$$

If material damping can be expressed as an exponential function of stress, as in Eq. (36.9), some significant generalizations can be made regarding the pronounced effect of the damping exponent n on each of these factors. Some of the results are shown in Fig. 36.8 for beams of constant cross-section. These curves indicate that high values of K_s and K_c are associated with a high damping exponent n , other factors being equal; K_c is high when very little material is near peak stress. For example, compare the diamond cross-section shape with the I beam, or compare the uniform stress beam with the cantilever.

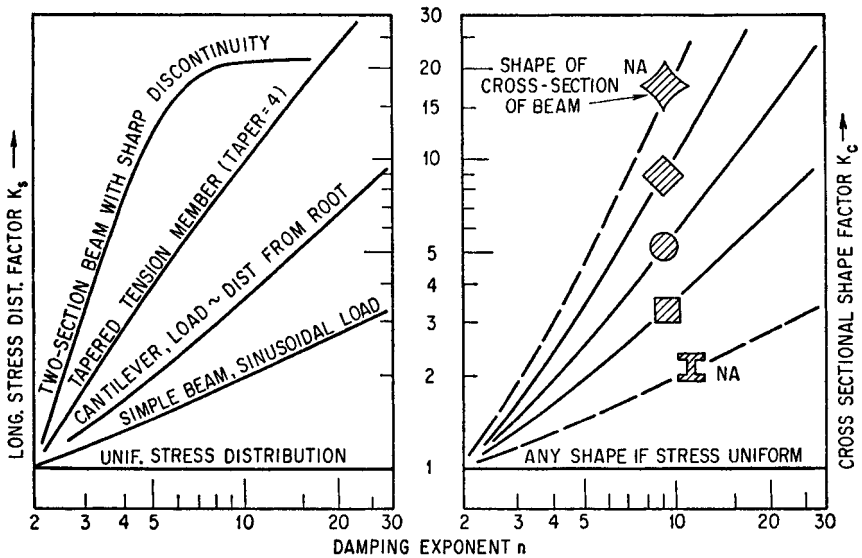


FIGURE 36.8 Effect of damping exponent n on longitudinal stress distribution factor and cross-sectional shape factor of selected examples.

In much of the literature on damping, the existence of the factors α and β (or K_s and K_c) is not recognized; the unstated assumption is that $\alpha = \beta = 1$. As discussed above, this assumption is true only for specimens under homogeneous stress.

Relative damping units such as logarithmic decrement depend on the ratio of two energies, the damping energy and the strain energy. Since strain energy increases with the square of the stress for reasonably linear materials, the logarithmic decrement remains constant with stress level and is independent of specimen shape and stress distribution only for materials whose damping energy also increases as the square of the stress [$n = 2$ in Eq. (36.9)]. For most materials at working stresses, n varies between 2 and 3 (see Fig. 36.10), but for some (Fig. 36.9) it is highly variable. In the high stress region, n lies in the range 8.0–20.0 (Fig. 36.10). In view of the broad range of materials and stresses encountered in design, the case $n = 2$ must be regarded as exceptional. Thus, logarithmic decrement is a variable rather than a “material constant.” Its magnitude generally decreases significantly with stress amplitude. When referring to specimens such as beams in which all stresses between zero and some maximum stress occur simultaneously, the logarithmic decrement is an ambiguous average value associated with some mean stress. Published data require careful analysis before suitable comparisons can be made.

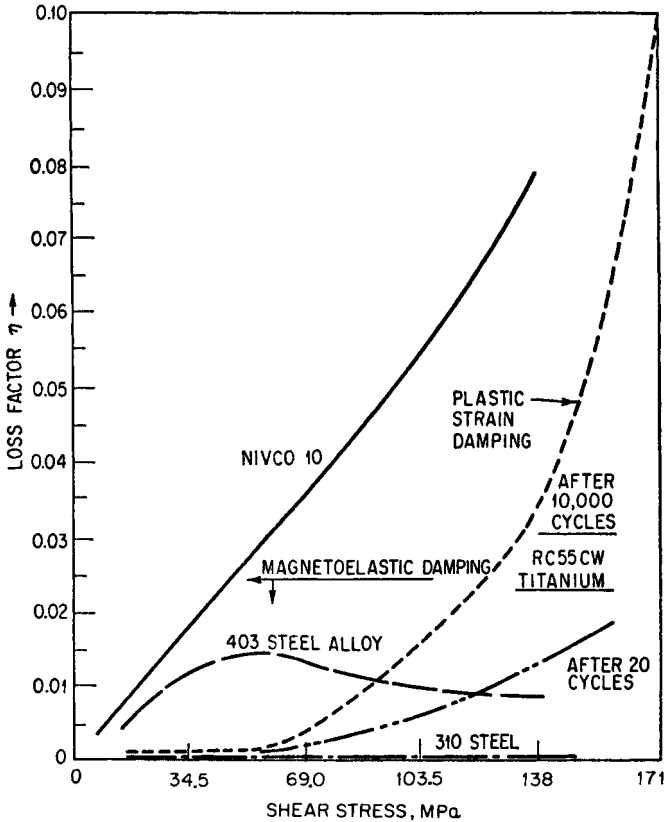


FIGURE 36.9 Comparison of internal friction and damping values for different inelastic mechanisms.

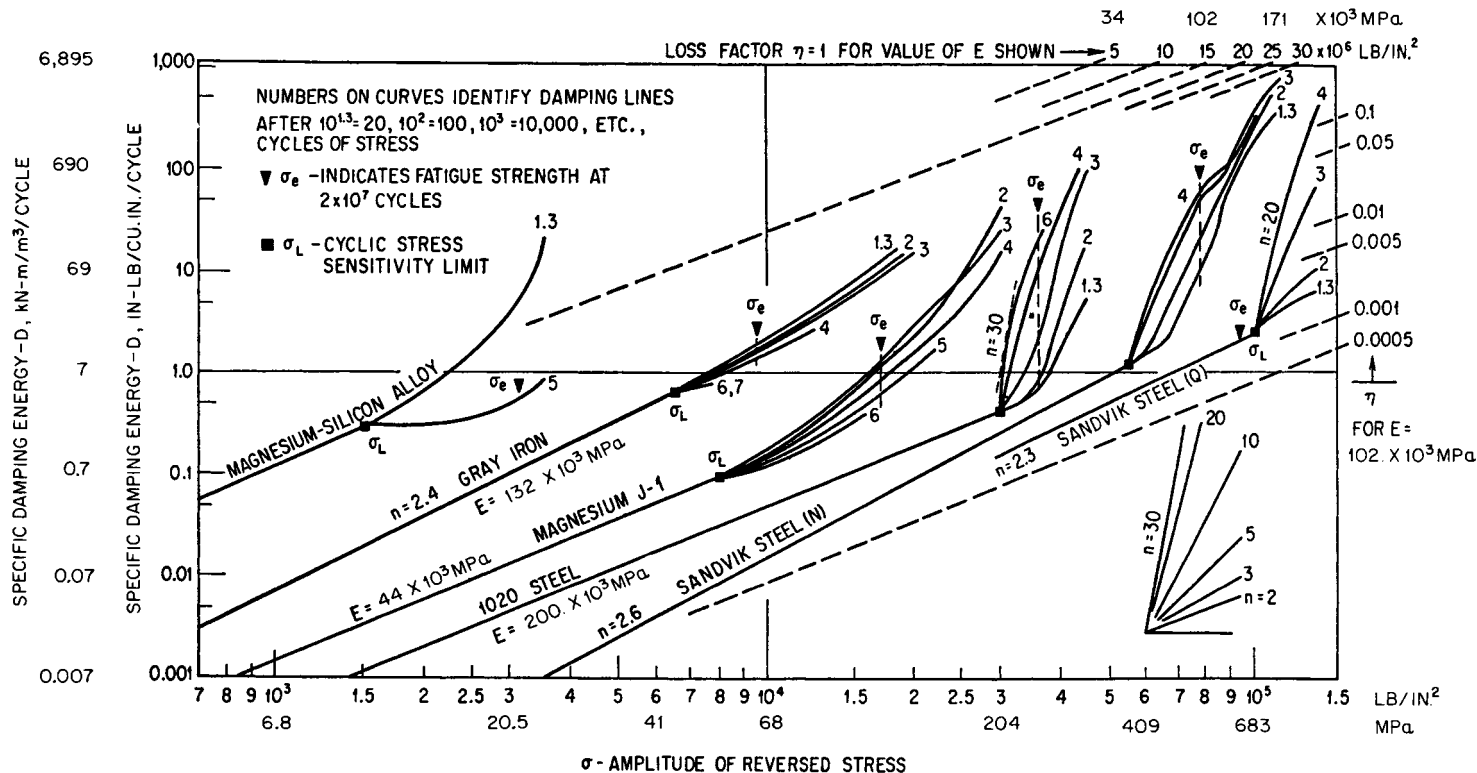


FIGURE 36.10 Specific damping energy of various materials as a function of amplitude of reversed stress and number of fatigue cycles. Number of cycles is 10 to power indicated on curve. For example, a curved marked 3 is for 10^3 or 1,000 cycles. Note: $6.895 \text{ kN-m/m}^3 = 1 \text{ in.-lb/in.}^3$ and $1 \text{ MPa} = 10^3 \text{ N/m}^2 = 10^{-3} \text{ kN/mm}^2 = 146.5 \text{ lb/in.}^2$.

VISCOELASTIC MATERIALS

Some materials respond to load in a way that shows a pronounced influence of the rate of loading. Generally the strain is larger if the stress varies slowly than it is if the stress reaches its peak value swiftly. Among materials that exhibit this viscoelastic behavior are high polymers and metals at elevated temperatures, as well as many glasses, rubbers, and plastics.¹³ As might be expected, these materials usually also exhibit creep, an increasing deformation under constant applied load.

When a sinusoidal exciting force is applied to a viscoelastic solid, the strain is observed to lag behind the stress. The phase angle between them, denoted by ϕ , is the *loss angle*. The stress may be separated into two components, one in phase with the strain and one leading it by a quarter cycle. The magnitudes of these components depend upon the material and upon the exciting frequency, ω . For a specimen subject to homogeneous shear ($\alpha = \beta = 1$),

$$\gamma = \gamma_0 \sin \omega t \quad (36.19)$$

$$\sigma = \gamma_0 [G'(\omega) \sin \omega t + G''(\omega) \cos \omega t] \quad (36.20)$$

This is a linear viscoelastic stress-strain law. The theory of linear viscoelasticity is the most thoroughly developed of viscoelastic theories. In Eq. (36.20), $G'(\omega)$ is known as the “storage modulus in shear” and $G''(\omega)$ is the “loss modulus in shear” (the symbols G_1 and G_2 are also widely used in the literature). The stiffness of the material depends on G' and the damping capacity on G'' . In terms of these quantities the loss angle $\phi = \tan^{-1}(G''/G')$. The *complex, or resultant, modulus in shear* is $G^* = G' + iG''$. In questions of stress analysis, complex moduli have the advantage that the form of Hooke’s law is the same as in the elastic case except that the elastic constants are replaced by the corresponding complex moduli. Then a correspondence principle often makes it possible to adapt an existing elastic solution to the viscoelastic case. For details of viscoelastic stress analysis, see Ref. 31.

The moduli of linear viscoelasticity are readily related to the specific damping energy D introduced previously. For a specimen in homogeneous shear of peak magnitude γ_0 , the energy dissipated per cycle and per unit volume is

$$D = \int_0^{2\pi/\omega} \sigma \left(\frac{d\gamma}{dt} \right) dt \quad (36.21)$$

In view of Eqs. (36.19) and (36.20) this becomes

$$\begin{aligned} D &= \int_0^{2\pi/\omega} \gamma_0^2 \omega (G' \sin \omega t + G'' \cos \omega t) \cos \omega t dt \\ &= \pi \gamma_0^2 G''(\omega) \end{aligned} \quad (36.22)$$

It is apparent from Eq. (36.22) that linear viscoelastic materials take the coefficient $n = 2$ in Eq. (36.9). These materials differ from metals, however, by having damping capacities that are strongly frequency- and temperature-sensitive.¹

DAMPING PROPERTIES OF MATERIALS

The specific damping energy D dissipated in a material exposed to cyclic stress is affected by many factors. Some of the more important are:

1. Condition of the material
 - a. In virgin state: chemical composition; constitution (or structure) due to thermal and mechanical treatment; inhomogeneity effects
 - b. During and after exposure to pretreatment, test, or service condition: Effect of stress and temperature histories on aging, precipitation, and other metallurgical solid-state transformations
2. State of internal stress
 - a. Initially, due to surface-finishing operations (shot peening, rolling, case hardening)
 - b. Changes caused by stress and temperature histories during test or service
3. Stress imposed by test or service conditions
 - a. Type of stress (tension, compression, bending, shear, torsion)
 - b. State of stress (uniaxial, biaxial, or triaxial)
 - c. Stress-magnitude parameters, including mean stress and alternating components; loading spectrum if stress amplitude is not constant
 - d. Characteristics of stress variations including frequency and waveform
 - e. Environmental conditions: temperature (magnitude and variation) and the surrounding medium and its (corrosive, erosive, and chemical) effects

Factors tabulated above, such as stress magnitude, history, and frequency, may be significant at one stress level or test condition and unimportant at another. The deformation mechanism that is operative governs the sensitivity to the various factors tabulated.

Many types of inelastic mechanisms and hysteretic phenomena have been identified, as shown in Table 36.2. The various damping phenomena and mechanisms may be classified under two main headings: *dynamic hysteresis* and *static hysteresis*.

Materials which display dynamic hysteresis (sometimes identified as viscoelastic, rheological, and rate-dependent hysteresis) have stress-strain laws which are describable by a differential equation containing stress, strain, and time derivatives of stress or strain. This differential equation need not be linear, though, to avoid mathematical complexity, much of the existing theory is based on the linear viscoelastic law described in the previous section. One important type of dynamic hysteresis, a special case identified as *anelasticity*^{14, 15} or *internal friction*, produces no permanent set after a long time. This means that if the load is suddenly removed at point *B* in Fig. 36.1, after cycle *OAB*, strain *OB* will gradually reduce to zero as the specimen recovers (or creeps negatively) from point *B* to point *O*.

A distinguishing characteristic of anelasticity and the more general case of viscoelastic damping is its dependence on time-derivative terms. The hysteresis loops tend to be elliptical in shape rather than pointed as in Fig. 36.1. Furthermore, the loop area is definitely related to the dynamic or cyclic nature of the loading and the area of the loop is dependent on frequency. In fact, the stress-strain curve for an ideally viscoelastic material becomes a single-valued curve (no hysteretic loop) if the cyclic stress is applied slowly enough to allow the material to be in complete equilibrium at all times (oscillation period very much longer than relaxation times). No hysteretic damping is produced by these mechanisms if the material is subjected to essentially static loading. Stated differently, the static hysteresis is zero.

Static hysteresis, by contrast, involves stress-strain laws which are insensitive to time, strain, or stress rate. The equilibrium value of strain is attained almost instantly for each value of stress and prior stress history (direction of loading, amplitudes, etc.), independent of loading rate. Hysteresis loops are pointed, as shown in Fig. 36.1, and if the stress is reduced to zero (point *B*) after cycle *OAB*, then *OB* remains as a permanent set or residual deformation. The two principal mechanisms which lead to static hysteresis are magnetostriction and plastic strain.

TABLE 36.2 Classification of Types of Hysteretic Damping of Materials


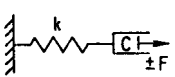
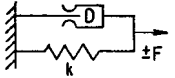
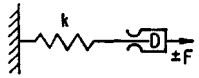
	Types of material damping		
Name used here	Dynamic hysteresis	Static hysteresis	
Other names	Viscoelastic, rheological, and rate-dependent hysteresis	Plastic, plastic flow, plastic strain, and rate-independent hysteresis	
Nature of stress-strain laws	Essentially linear. Differential equation involving stress, strain, and their time derivatives	Essentially nonlinear, but excludes time derivatives of stress or strain	
Special cases and description	<i>Anelasticity</i> . Special because no permanent set after sufficient time. Called “internal friction”		
Simplest representative mechanical model	<p>VOIGT UNIT</p>  <p>ANELASTICITY</p> <p>MAXWELL UNIT</p> 	 	
Frequency dependence	Critically at relaxation peaks	No, unless other mechanisms present	
Primary mechanisms	Solute atoms, grain boundaries. Micro- and macro-thermal and eddy currents. Molecular curling and uncurling in polymers.	Magnetoelasticity	Plastic strain
Value of n in $D = JS^n$	2	3—up to coercive force	2–3 up to σ_L 2 to >30 above σ_L
Variation of η with stress	No change, since $n - 2 = 0$	Proportional to σ since $n - 2 = 1$	Small increase up to σ_L Large increase above σ_L
Typical values for η	Anelasticity: <0.001 to 0.01 Viscoelasticity: <0.1 to >1.5	0.01 to 0.08	0.001 to 0.05 up to σ_L 0.001 to >0.1 above σ_L
Stress range of engineering importance	Anelasticity—low stress Viscoelasticity—all stresses	Low and medium. Sometimes high	Medium and high stress
Effect of fatigue cycles	No effect	No effect	No effect up to σ_L Large changes above σ_L
Effect of temperature	Critical effects near relaxation peaks	Damping disappears at Curie temperature	Mixed. Depends on type of comparison
Effect of static preload		Large reduction for small coercive force	Either little effect or increase

Table 36.2 also shows the simplest representative mechanical models for each of the behaviors classified. In these models, k is a spring having linear elasticity (linear and single-valued stress-strain curve), C is a linear dashpot which produces a resisting force proportional to velocity, and D is a Coulomb friction unit which produces a constant force whenever slip occurs within the unit, the direction of the force being opposite to the direction of relative motion. More sophisticated models have been found to predict reliably the behavior of some materials, particularly polymeric materials.

Any one of the mechanisms to be discussed may dominate, depending on the stress level. For convenience, *low stress* is defined here as a (tension-compression) stress less than 1 percent of the fatigue limit; *intermediate* stress levels are those between 1 percent and 50 percent of the fatigue limit of the material; and *high* stress levels are those exceeding 50 percent of the fatigue limit.

DYNAMIC HYSTERESIS OF VISCOELASTIC MATERIALS

The linearity limits of a variety of plastics and rubbers are summarized in Table 36.3. While the stress limits are of the same order of magnitude for plastics and rubbers, the strain limits are much smaller for the former class of materials. Within these limits the dynamic storage and loss moduli of linear viscoelasticity may be used.

One distinguishing characteristic of the dynamic behavior of viscoelastic materials is a strong dependence on temperature and frequency.^{1,16} At high frequencies (or low temperature) the storage modulus is large, the loss modulus is small, and the behavior resembles that of a stiff ideal material. This is known as the “glassy” region in which the “molecular curling and uncurling” cannot occur rapidly enough to fol-

TABLE 36.3 Linearity Limits for a Variety of Plastics and Rubber

Material	Stress limit in creep, MPa	Strain limit in relaxation
Polymethylmethacrylate	10	
Polystyrene	5	
Plasticized polyvinyl chloride	1	0.1–1.0%
Polythene	12	
Phenolic resins	10	
Polyisobutylene		$\left\{ \begin{array}{l} 50\% \\ 100\% \\ 100\% \end{array} \right.$
Natural rubber	1–10	
GR-S		

Note: 1 MPa = 10^6 N/m² = 146.5 lb/in.².

low the stress. Thus the material behaves essentially “elastically.” At low frequencies (or high temperature) the storage modulus and the loss modulus are both small. This is the “rubbery” region in which the molecular curling and uncurling follow the stress in phase, resulting in an equilibrium condition not conducive to energy dissipation. At intermediate frequencies and temperatures there is a “transition” region in which the loss modulus is largest. In this region the molecular curling and uncurling is out of phase with the cyclic stress and the resulting lag in the cyclic strain provides a mechanism for dissipating damping energy. The loss factor also shows a peak

in this region, although at a somewhat lower frequency than the peak in G'' . Since the damping energy is proportional to G'' , the specific damping curve also has its maximum in the transition region. Most engineering problems involving vibration are associated with the transition and glassy regions. In Table 36.4, values of G' and G'' are given for a variety of rubbers and plastics. References 17 to 20 contain additional useful information.

Metals at low stress exhibit certain properties that constitute dynamic hysteresis effects. Peaks are observed in curves of loss factors vs. frequency of excitation. For example, under conditions that maximize the internal friction associated with grain boundary effects, polycrystalline aluminum will display a loss factor peak as high as $\eta = 0.09$. But for most metals, the peak values are less than 0.01. Although the rheo-

TABLE 36.4 Typical Moduli of Viscoelastic Materials

(Two values are given: the upper value is G' ; the bottom value is G'' . Moduli units are megapascals, MPa.)

Material	Frequency, Hz				Temperature, °C
	10	100	1000	4000	
Polyisobutylene		0.512	1.31	2.36	-60-100
		0.410	1.76	4.50	
M 169A Butyl gum		0.480	1.40	2.70	21-65
		0.502	1.32	2.88	
Du Pont fluoro rubber, (Viton A)		2.00	4.54	7.93	0-100
		1.60	8.41	27.0	
Silicon rubber gum		0.05	0.08		21-65
		0.02	0.04		
Natural rubber		0.33	0.50		25
		0.02	0.02		
3M tape No. 466 (adhesive)		0.81	2.52	15.3	25
		0.95	4.59	13.0	
3M tape No. 435 (sound damping tape)		0.28	0.55	0.87	-40-60
		0.16	0.37	0.63	
Natural rubber (tread stock)	3.91	4.91			-30-75
	0.68	0.97			
Thiokol M-5	7.86	8.34			-30-75
	3.91	10.27			
Natural gum (tread stock)	0.73				-30-75
	0.07				
Filled silicone rubber		2.00	2.50	3.41	21-65
		0.26	0.44	0.58	
Polyvinyl chloride acetate		1.26	3.20	6.60	21-65
		1.44	2.32	5.78	
X7 Polymerized tung oil with polyoxane liquid			17.0	39.0	21-65
			9.45	20.8	
Du Pont X7775 pyralin	4.50	12.0	45.0		-45-100
	2.51	9.45	28.3		
Polyvinyl butyral	30.0	200.0	600.0		-45-100
	3.1	12.5	37.6		
Polyvinyl chloride with dimethyl thianthrene		0.35	0.65		
		0.21	0.97		

Note: 1 MPa = 10^6 N/m² = 10^{-3} kN/mm² = 146.5 lb/in.².

logical properties of metals at low stress can be described in terms of anelastic properties (rheology without permanent set), a more general approach which includes provisions for permanent set is required to specify the rheological properties of metals at high stress. This approach is best described in terms of static hysteresis.

STATIC HYSTERESIS

The metals used in engineering practice exhibit little internal damping at low stress levels. At intermediate and high stress levels, however, magnetostriction and plastic strain can introduce appreciable damping. The former effect is considered first.

Ferromagnetic metals have significantly higher damping at intermediate stress levels than do nonferromagnetic metals. This is because of the rotation of the magnetic domain vectors produced by the alternating stress field. If the specimen is magnetized to saturation, most of the damping disappears, indicating that it was due primarily to magnetoelastic hysteresis. Figure 36.9 shows the loss factor for three metals, each heat-treated for maximum damping. The damping of 403 steel (ferromagnetic material with 12% Cr and 5% Ni) is much higher than that of 310 steel (nonferromagnetic with 25% Cr and 20% Ni). Most structural metals at low and intermediate stress exhibit loss factors in the general range of 310 steel until the hysteresis produced by plastic strain becomes significant. The alloy Nivco 10²¹ (approximately 72% Co and 23% Ni), developed to take maximum advantage of magnetoelastic hysteresis, displays significantly larger damping than other metals.

The damping energy dissipated by magnetoelastic hysteresis increases as the third power of stress up to a stress level governed by the magnetomechanical coercive force; thus, the loss factor should increase linearly with stress. Nivco 10 follows this relationship for the entire range of stress shown in Fig. 36.9. Beyond an alternating stress governed by the magnetomechanical coercive force, i.e., beyond approximately 34.5 MPa (5,000 lb/in.²) for the 403 steel, the damping energy dissipated becomes constant. Since the elastic energy W_0 continues to increase as the square of the alternating stress, the value of loss factor (ratio of the two energies) decreases with the inverse square of stress. The curve for 403 steel in Fig. 36.9 at stresses between 62 MPa (9,000 lb/in.²) and 103 MPa (15,000 lb/in.²) demonstrates this behavior.

Magnetoelastic damping is independent of the excitation frequency, at least in the frequency range that is of engineering interest. Magnetoelastic damping decreases only slightly with increasing temperature until the Curie temperature is reached, when it decreases rapidly to zero. Static stress superposed on alternating stress reduces magnetoelastic damping.^{21,22}

It is not entirely clear what mechanisms are encompassed by the terms plastic strain, localized plastic deformation, crystal plasticity, and plastic flow in a range of stress within the apparent elastic limit. On the microscopic scale, the inhomogeneity of stress distribution within crystals and the stress concentration at crystal boundary intersections produce local stress high enough to cause local plastic strain, even though the average (macroscopic) stress may be very low. The number and volume of local sites so affected probably increase rapidly with stress amplitude, particularly at stresses approaching the fatigue limit of a material. On the submicroscopic scale, the role of dislocations, their kind, number, dispersion, and lattice anchorage in the deformation process still remains to be determined. The processes involved in these various inelastic behaviors may be included under the general term "plastic strain."

At small and intermediate stress, the damping caused by plastic strain is small, probably of the same order as some of the internal friction peaks discussed previ-

ously and much smaller than magnetoelastic damping in many materials. In this stress region, damping generally is not affected by the stress or strain history. However, as the stress is increased, the plastic strain mechanism becomes increasingly important and at stresses approaching the fatigue limit it begins to dominate as a damping mechanism. This is shown by the curves for titanium in Fig. 36.9.²² In the region of high stress, microstructural changes and metallurgical instability appear to be initiated and promoted by cyclic stress. This occurs even though the stress amplitude may lie below the apparent elastic limit (that observed by conventional methods) and the fatigue limit of the material. This means that damping in the high stress region is a function not only of stress amplitude but also of stress history. In Fig. 36.9, for example, the lower of the two curves for titanium indicates the damping of the virgin specimen and the upper curve gives the damping after 10,000 stress cycles.

The general position as regards stress history is given in Fig. 36.10. Below a certain peak stress, σ_L , known as the “cyclic stress sensitivity limit,” the curve of damping vs. stress is a straight line on a log-log plot and displays no stress-history effect. The limit stress σ_L usually falls somewhat below the fatigue strength of the material. Above σ_L , stress-history effects appear; the curve labeled 1.3 indicates the damping energy after $10^{1.3} = 20$ cycles and the curve labeled 6 after 10^6 or 1 million cycles. To facilitate comparisons between the reference damping units, loss factor η and D under uniform stress ($\alpha/\beta = 1$), the loss factor also is plotted in Fig. 36.10. Since the relationship between D and η depends on the value of Young’s modulus of elasticity E , a family of lines for the range of $E = 34 \times 10^3$ to 205.0×10^3 MPa (5×10^6 to 30×10^6 lb/in.²) is shown for $\eta = 1$. The lines for the other values of η correspond to a value of $E = 102.0 \times 10^3$ MPa (15×10^6 lb/in.²).

TABLE 36.5 Static, Hysteretic, Elastic, and Fatigue Properties of a Variety of Metals

Material*	Static properties			Fatigue behavior		
	Modulus of elasticity E , MPa 10^{-4}	Yield stress (0.2% offset), MPa	Tensile strength, MPa	Fatigue strength σ_e , MPa	Cyclic stress sensitivity limit σ_L , MPa	Stress ratio σ_L/σ_e
N-155 (superalloy)	20.	410.	810.	360.	220.	0.62
Lapelloy (superalloy)	22.	764.	880.	490.	490.	1.00
Lapelloy (480°C)	17.5			270.	310.	1.14
RC 130B (titanium)	11.5	950.	1,040.	590.	650.	1.10
RC 130B (320°C)	9.9			430.	340.	0.81
Sandvik (O & T) steel	19.9	1,210.	1,400.	630.	680.	1.09
SAE 1020 steel	20.1	320.	490.	240.	200.	0.85
Gray iron	13.2		140.	65.	44.	0.69
24S-T4 aluminum	7.2	330.	500.	180.	160.	0.88
J-1 magnesium	4.4	230.	310.	120.	55.	0.47
Manganese-copper alloy		410.	610.	130.	120.	0.95

Note: 1 MPa = 10^6 N/m² = 146 lb/in.².
 (Includes test temperature if above room temperature.)

COMPARISON OF VARIOUS MATERIAL DAMPING MECHANISMS AND REPRESENTATIVE DATA FOR ENGINEERING MATERIALS

The general qualitative characteristics of the various types of damping are summarized in Table 36.2 by comparing the effects of different testing variables. The data tabulated indicate that, in general, anelastic mechanisms do not contribute significantly to total damping at intermediate and high stresses; in these regions magnetoelastic and plastic strain mechanisms probably are the most important from an engineering viewpoint.

Damping vs. stress ratio data have been determined for a variety of common structural materials at various temperatures.^{2,4} Some of these data are listed in Table 36.5 (all tests at 0.33 Hz). For a large variety of structural materials (not particularly selected for large magnetoelastic or plastic strain damping), the data are found to lie within a fairly well-established band shown in Fig. 36.11. The approximate geometric-mean curve is shown. Up to the fatigue limit, that is up to $\sigma_d = \sigma_e$, the specific damping energy D is given with sufficient accuracy by the expression

$$D = J \left(\frac{\sigma}{\sigma_e} \right)^{2.4} \tag{36.23}$$

where $J = 6.8 \times 10^{-3}$ if D is expressed in SI units of MN·m/m³/cycle, and the value of $J = 1.0$ if D is expressed in units of in.-lb/in.³/cycle.

The approximate bandwidth about the geometric mean curve in Fig. 36.11 for the various structural materials included in the band is as follows: from 1/3 to 3 times the mean value at a stress ratio of 0.2 or less; from 1/5 to 5 times at a ratio of 0.6; from 1/10 to 10 times at a ratio of 1.0.

Damping properties, kN·m/m ³ /cycle							
$D = J \left(\frac{\sigma}{\sigma_e} \right)^n$				D at $\sigma/\sigma_e = 1$		D at $\sigma/\sigma_e = 1.2$	
$\sigma \leq \sigma_L$				After	After	After	Maximum
J	n , dimensionless	$\frac{D}{\sigma_L}$	$\frac{D}{\sigma_e}$	10 ^{1.3} cycles	10 ⁶ cycles	10 ^{1.3} cycles	number of cycles
8.8	2.5	2.7	2.7	310.	170.	1,230.	1,500.
30.*	2.4*	10.9	4.0	11.	11.	55.	170.
24.	2.2	34.	8.2	26.	26.	41.	48.
14.	2.0	14.	4.4	12.	12.	18.	24.
17.	1.9	12.	6.1	13.	34.	30.	170.
16.	2.3	19.	5.5	16.	16.	31.	200.
4.3	2.0	3.1	1.6	4.5	140.	34.	680.
12.	2.4	4.5	3.4	14.	8.2	22.	16.
3.9	2.0	3.0	1.4	6.8	4.1	6.	15.
3.1	2.0	0.7	0.9	7.5	3.4	24.	7.
96.	2.8	82.	22.	89.	89.	170.	140.

Note: 1 kN·m/m³/cycle = 0.146 in.-lb/in.³/cycle.

* Up to $\sigma = 96$ MPa (14,000 lb/in.²); at $\sigma = 204$ MPa (30,000 lb/in.²) $n = 1.5$.

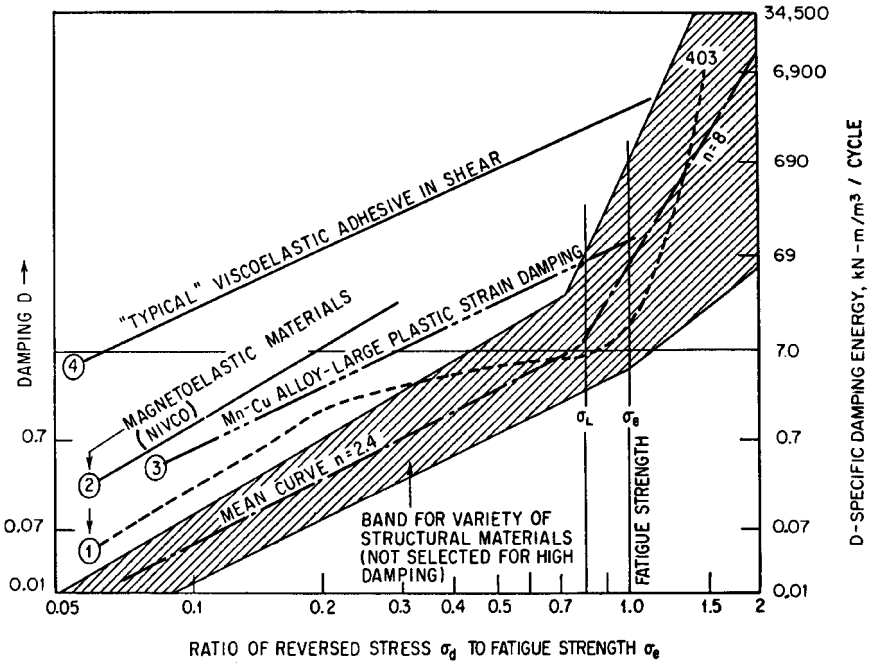


FIGURE 36.11 Range of damping properties for a variety of structural materials. The shaded band defines the damping for most structural materials. 1 kN·m/m³ = 0.146 in.-lb/in.³.

Also shown in Fig. 36.11 for comparison purposes are data for four materials having especially high damping. Materials 1 and 2 are the magnetoelastic alloys Nivco 10 and 403. Nivco 10 retains its high damping up to the stresses shown (data not available at higher stresses). However, the 403 alloy reaches its magnetoelastic peak at a stress ratio of approximately 0.2 and increases less rapidly beyond this point; when plastic strain damping becomes dominant (at stress ratio of approximately 0.8), damping increases very rapidly. By contrast, material 3, a manganese-copper alloy with large plastic strain damping, retains its high damping up to and beyond its fatigue strength.²³ Material 4 is a “typical” viscoelastic adhesive ($G'' = 0.95 \text{ MPa} = 138 \text{ lb/in.}^2$), assuming that the permissible cyclic shear strain is unity (experiments show that a shear strain of unity does not cause deterioration in this adhesive even after millions of cycles).²⁴ The magnetoelastic material has a damping thirty times as large as the average structural material in the stress range shown in Fig. 36.11, and the viscoelastic damping is over ten times as large as the magnetoelastic damping.

The range of D observed for common structural materials stressed at their fatigue limit is 0.003 to 0.7 MN·m/m³/cycle with a mean value of 0.05 (0.5 to 100 in.-lb/in.³/cycle with a mean value of 7). For materials stressed at a rate of 60 Hz under a uniform stress distribution (tension-compression), 16.4 cm³ (1 in.³) of a typical material will safely absorb and dissipate 48 watts (0.064 hp). Some high damping materials can absorb almost 746 watts (1 hp) in the safe-stress range, assuming no significant frequency or stress-history effects.²⁵⁻²⁷

SLIP DAMPING

In some cases the hysteretic damping in a structural material is sufficient to keep resonant vibration stresses within reasonable limits. However, in many engineering designs, material damping is too small and structural damping must be considered. A structural damping mechanism which offers excellent potential for large energy dissipation is that associated with the interface shear at a structural joint.

The initial studies²⁸⁻³⁰ on interface shear damping considered the case of Coulomb or dry friction. Under optimum pressure and geometry conditions, very large energy dissipation is possible at a joint interface. However, the application of the general concepts of optimum Coulomb interface damping to engineering structures introduces two new problems. First, if the configuration is optimum for maximum Coulomb damping, the resulting slip can lead to serious corrosion due to chafing; this may be worse than the high resonance amplification associated with small damping. Second, for many types of design configurations, the interface pressure or other design parameters must be carefully optimized initially and then accurately maintained during service; otherwise, a small shift from optimum conditions may lead to a pronounced reduction in total damping of the configuration. Since it usually is difficult to maintain optimum pressure, particularly under fretting conditions, other types of interface treatment have been developed. One approach is to lubricate the interface surfaces. However, the maintenance of a lubricated surface often is difficult, particularly under the large normal pressure and shear sometimes necessary for high damping. Therefore, a more satisfactory form of interface treatment is an adhesive separator placed between mating surfaces at an interface. The function of the separating adhesive layer is to distort in shear and thus to dissipate energy with no significant Coulomb friction or sliding and therefore no fretting corrosion. The design of such layers is discussed in Chap. 37.

DAMPING BY SLIDING

The nature of interface shear damping can be explained by considering the behavior of two machine parts or structural elements which have been clamped together. The clamping force, whether it is the result of externally applied loads, of accelerations present in high-speed rotating machinery, or of a press fit, produces an interface common to the two parts. If an additional exciting force F_g is now gradually imposed, the two parts at first react as a single elastic body. There is shear on the interface, but not enough to produce relative slip at any point. As F_g increases in magnitude, the resulting shearing traction at some places on the interface exceeds the limiting value permitted by the friction characteristics of the two mating surfaces. In these regions microscopic slip of adjacent points on opposite sides of the interface occurs. As a result, mechanical energy is converted into heat. If the mechanical energy is energy of free or forced vibration, damping occurs. The slipped region is local and does not, in general, extend over the entire interface. If it does extend over the entire interface, gross slip is said to occur. This usually is prevented by the geometry of the system.

The force-displacement relationship for systems with interface shear damping is shown in Fig. 36.12. Since there are many displacements which can be measured, the displacement which corresponds to the exciting force that acts on the system is taken as a basis. Then the product of displacement and exciting force, integrated over a complete cycle, is the work done by the exciting force and absorbed by the structural element. As shown in Fig. 36.12, there is an initial linear phase OP during which behavior is entirely elastic. This is followed, in general, by a nonlinear transi-

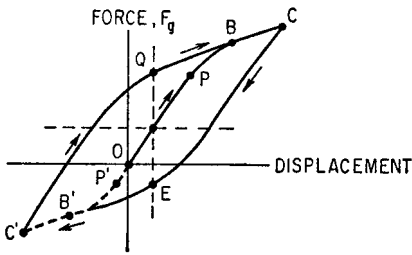


FIGURE 36.12 Force-displacement hysteresis loop under Coulomb friction.

allowed to exceed the value corresponding to point *B*. If it should exceed this gross value, slip would occur.

If the clamping force itself does not produce any shear on the interface and if the exciting force does not affect the clamping pressure, the force-displacement curve is symmetrical about the origin *O*. These conditions are at least approximately fulfilled in many cases. If they are not fulfilled, the exciting force in one direction initiates slip at a different magnitude of load than the exciting force in the opposite direction. This is the case pictured in Fig. 36.12. With negative exciting force, slip is initiated at *P'* which corresponds to a force of considerably smaller magnitude than point *P*. However, the force-displacement curve is always symmetrical about the mid-point of *PP'* (intersection of dashed lines in Fig. 36.12).

The force-displacement curve has been followed from point *O* to point *C*. If now a reduction in the exciting force occurs, the curve proceeds from *C* in a direction parallel to its initial elastic phase. Eventually, as unloading proceeds, slip is initiated again. Its sense is now opposite to that which was produced by positive force. The curve continues to point *B'*, where slip is complete, and then along a linear stretch to *C'*, where the exciting force has its largest negative value. As the force reverses, the curve becomes again linear and parallel to *OP*. Slip eventually occurs again and covers the interface at *B*. The hysteresis loop is closed at *C*.

The energy dissipated in local slip can be found by computing the area enclosed by the force-displacement hysteresis loop. It usually is simpler, however, to determine the energy loss at a typical location on the interface by analysis, and then to integrate over the area of the interface. In this mode of procedure, interest centers on the frictional force per unit area $\mu\sigma$ and the relative displacement Δs of initially adjacent points on opposite sides of the interface.

The so-called "slip-curve" illustrating the relationship between $\mu\sigma$ and Δs is shown in Fig. 36.13. Before the exciting

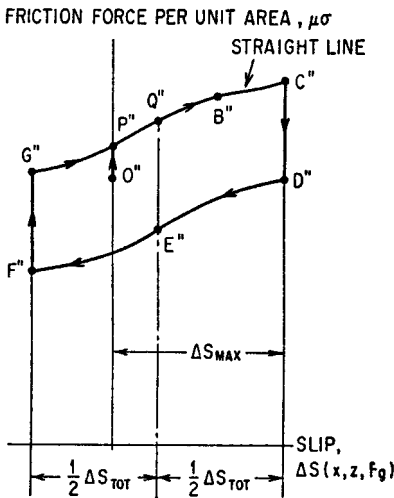


FIGURE 36.13 Friction force-slip relationship under Coulomb friction.

force is applied, conditions are represented by point O'' which corresponds to point O in Fig. 36.12. The initial elastic phase during which there is no slip is represented by $O''P''$ (note that the normal pressure σ may change during this phase). The phase during which slip occurs only over part of the interface is represented by the curved line $P''B''$; it corresponds to PB in Fig. 36.12. After slip has progressed over the entire interface, the normal force vs. relative-displacement relation is linear. This phase is represented by the curve $B''C''$ in Fig. 36.13 and by BC in Fig. 36.12. When the exciting force has reached its maximum value, a second nonslip phase $C''D''$ ensues. This is followed by slip along the curve $D''E''F''$ until the exciting force reaches its maximum negative value. As the exciting force completes its period, there is a nonslip phase $F''G''$ followed by slip along $G''C''$. The lengths $C''D''$ and $F''G''$ are equal and the curves $G''C''$ and $D''F''$ are congruent (F'' corresponds to C'' and D'' corresponds to G'').

If the point in question is at an element of area $dx dz$ of the xz interface, the energy dissipated in slip is proportional to the area enclosed by the slip curve. Because of the congruence of the curved portions of the diagram and the parallelism of the linear portions, this area can be expressed in terms of the total slip and the pressures at two instants during the loading cycle. Integrating over the entire interface,

$$D_0 = -\mu \int \int [\sigma(E'') + \sigma(Q'')] \Delta s_{\text{tot}} dx dz \tag{36.24}$$

In this expression, the parameters $\sigma(E'')$ and $\sigma(Q'')$ and the total slip Δs_{tot} are functions of x and z . They are the normal stresses at points E'' and Q'' in Fig. 36.13, located midway between the vertical lines $G''F''$ and $C''D''$. Since the pressures σ are always compressive (negative) and the total slip is always taken as a positive quantity, the negative sign is required to ensure a positive energy dissipation. Equation (36.24) is of little engineering value in itself because the stresses are functions of F_g as well as of x and z . In many of the problems which are of design interest, however, the shear on the interface is produced primarily by the exciting force and not by the initial clamping pressure. Conversely, the clamping pressure is not greatly affected by the addition of the time-varying exciting force. Under these circumstances, the slip curve of Fig. 36.13, like the force-displacement curve of Fig. 36.12, is symmetric about the point O'' . Points P'' and Q'' then coincide, and the mean ordinate of the slip curve is that corresponding to point O'' . Then Eq. (36.24) reduces to

$$D_0 = -4\mu \int \int \sigma(O'') \Delta s_{\text{max}} dx dz \tag{36.25}$$

where $\sigma(O'')$ is the clamping stress corresponding to zero exciting force. It may be determined by any of the well-known methods of stress analysis. In most cases, $\sigma(O'')$ can be determined without any reference to the existence of an interface. The term Δs_{max} represents the arc length of the maximum relative displacement, the so-called "scratch path." It is a function of the maximum value of F_g as well as of position on the interface. It may be inferred from Eq. (36.25) that energy dissipation due to interface shear is small both at very low clamping pressures and at very high ones. In the former case, $\sigma(O'') = 0$; in the latter case, $\Delta s_{\text{max}} = 0$. It follows that, for any distribution of clamping pressure, there is an optimum intensity of clamping force at which the energy dissipation due to interface shear is a maximum. The maintenance of this optimum pressure is essential to the utilization of this form of damping. From the shape of the force-displacement curve $OPBC$ shown in Fig. 36.12, it is evident that systems in which interface shear damping plays a significant role behave like softening springs. This means that instability and jump phenomena may occur at frequencies below the nominal resonant frequency.

In the case of plane stress, the thickness of the material is t and Eq. (36.25) becomes

$$D_0 = -4\mu t \int \sigma(O'') \Delta s_{\max} dx \quad (36.26)$$

The slip can be related to stress through Hooke's law:

$$\Delta s = E^{-1} \int (\Delta \sigma_x) dx \quad (36.27)$$

This indicates that any discontinuity in displacement is associated with a discontinuity in the component of stress parallel to the interface. These displacement discontinuities due to slip are members of a class of generalized dislocations whose existence has been demonstrated theoretically.³² If Eq. (36.27) is substituted in Eq. (36.26), the energy dissipation can be expressed in terms of stress alone:

$$D_0 = -4\mu E^{-1} t \int_0^l \sigma(O'') \left[\int_0^x (\Delta \sigma_x)_{\max} dx' \right] dx \quad (36.28)$$

The computation of energy dissipation per cycle D_0 is the first step in the prediction of the dynamic amplification factor to be expected in service. For interface shear damping, an elementary theory permits the dynamic amplification factor to be estimated even though the system behavior is nonlinear. The technique employs an averaging method. Denoting the displacement corresponding to the exciting force by the symbol v ,

$$v = v_d \cos \omega t \quad \text{and} \quad F_g = F_m \cos (\omega t + \varphi) \quad (36.29)$$

where v_d is the peak dynamic displacement, F_m is the peak exciting force, and φ is the loss angle. One relationship between these quantities is obtained by making the average value of the virtual work vanish during each half-cycle of the steady-state forced vibration:

$$\int_0^{\pi/\omega} [mv + kv - F_g] \cos \omega t dt = 0 \quad (36.30)$$

In this integration, the stiffness k changes as slip progresses across the interface. If the hysteresis loop of Fig. 36.12 is replaced by a parallelogram, only two phases, elastic and fully slipped, need be considered. Denoting the stiffness (i.e., the ratio of exciting force to displacement) in the unslipped condition by the symbol k_e and the reduced stiffness in the fully slipped condition by the symbol k_s , the phase angle φ and the dynamic amplification factor A may be related by Eq. (36.30) to the duration of the elastic phase t' :

$$\left(1 - \frac{k_s}{k_e}\right) (\omega t' + \sin \omega t') = \pi \left(\frac{m\omega^2 k_s}{k_e} + \frac{\cos \varphi}{A} \right) \quad (36.31)$$

where A is the conventional dynamic amplification factor, i.e., $A = v_d k_e / F_m$. The duration of the elastic phase is given by the first of Eqs. (36.29) with $v = v_d - 2v_s$, where v_s is the displacement at which slip first occurs. Then eliminating t' from Eq. (36.31):

$$\frac{\cos \varphi}{A} = \frac{1}{\pi} \left(1 - \frac{k_s}{k_e}\right) \left[2 \frac{v_s k_e}{AF_m} \sqrt{1 + \frac{v_s k_e}{AF_m}} + \cos^{-1} \left(1 - 2 \frac{v_s k_e}{AF_m}\right) \right] - \frac{m\omega^2 k_s}{k_e} \quad (36.32)$$

Equation (36.32) gives the relation between phase lag φ and amplification factor A . A second relationship between these quantities is found from the consideration that the energy dissipated during each half cycle of forced motion must be $D_0/2$:

$$\int_0^{\pi/\omega} F_g \frac{dv}{dt} dt = \frac{1}{2} D_0 \quad \text{or} \quad \sin \varphi = \frac{D_0 k_e}{\pi F_m^2 A} \quad (36.33)$$

Equations (36.32) and (36.33) serve to determine the dynamic amplification factor A , after D_0 has been estimated. Conversely, they serve to estimate the amount of energy which must be dissipated per cycle to produce a given reduction in the amplification factor by interface shear. A detailed analysis of the response to a parallelogram hysteresis loop has been made.³³ Hysteresis loops other than parallelograms also have been studied.³⁴ At resonance, $\phi = 90^\circ$ and

$$A = A_r = \frac{D_0 k_e}{\pi F_m^2} \quad (36.34)$$

In general, the energy dissipation does not increase as rapidly as the square of the peak exciting force; consequently, the resonance amplification factor decreases as the exciting force increases. As a result, structures in which interface shear predominates tend to be self-limiting in their response to an external excitation.

The foregoing discussion is based on the premise that changes in the exciting force do not materially affect the size of the contact area. There is an important class of problems for which this assumption is not valid, namely, those in which even the smallest exciting force produces some slip. An example of this type of joint is the press-fit bushing on a cylindrical shaft. If the ends of the shaft are subjected to a cyclic torque, part of this torque is transmitted to the bushing. Each part of the compound torque tube carries a moment proportional to its stiffness. Transmission of torque from the shaft to the bushing is effected by slip over the interface. The length of the slipped region grows in proportion to the applied torque. There is no initial elastic region such as OP or $O'P'$ in Figs. 36.12 and 36.13. If the peak value of the exciting torque is not too large, the fully slipped region BC or $B'C'$ in Fig. 36.12 never occurs. In these cases, Eqs. (36.31) to (36.34) are not applicable because there are no assignable constant values of k_s and k_e . A variety of simple cases of this type which occur in design practice have been analyzed. They include the cylindrical shaft and bushing in tension and torsion, and the flexure of a beam with cover plate.

Another important case in which the smallest exciting force may produce slip arises in the contact of rounded solids. If these are pressed together by normal forces along the line joining their centers, a small contact region is formed. Subsequent application of a cyclic tangential force produces slip over a portion of the contact region even if the peak tangential force is not great enough to effect gross slip or sliding. This situation has been analyzed and verified experimentally.^{3,36}

REFERENCES

1. Alfrey, T., Jr.: "Mechanical Behavior of High Polymers," Interscience Publishers, Inc., New York, 1948.
2. Lazan, B. J.: "Damping of Materials and Members in Structural Mechanics," Pergamon Press, New York, 1968.
3. Johnson, K. L.: "Contact Mechanics," Cambridge University Press, 1985.
4. Lazan, B. J.: "Fatigue," chap. II, American Society for Metals, 1954.
5. Cochartd, A. W.: *J. Appl. Mechanics*, **21**:257 (1954).
6. Lazan, B. J.: *Trans. ASME*, **65**:87 (1943); Pisarenko, G. S.: "Vibrations of Mechanical Systems Taking into Account Incompletely Elastic Materials," 2d ed., Kiev, 1970 (in Russian).
7. Von Heydekampf, G. S.: *Proc. ASTM*, **31** (Pt.II):157 (1931); Jones, D. I. G., and D. K. Rao: *ASME Des. Div. Pub. DE*, **5**:143 (1987).

8. Lazan, B. J.: *Trans. ASM*, **12**:499 (1950).
9. Maxwell, B.: *ASTM Bull.*, **215**:76 (1956).
10. Nowick, A. S.: "Progress in Metal Physics," vol. 4, chap. I, p. 29, Interscience Publishers, Inc., New York, 1953; Tschan, T., et al.: *Proc. Euroensors V, Sensors and Actuators, A: Physical*, **32**, n.1-3:375 (1992); Kalachnikov, E. V., and P. N. Rostovstev: *Instr. Exp. Tech.*, **32**:1241 (1990).
11. Podnieks, E., and B. J. Lazan: *Wright Air Development Center Tech. Rep.* 55-284, 1955.
12. Lazan, B. J.: *J. Appl. Mechanics*, **20**:201 (1953).
13. Lakes, R. S.: "Viscoelastic Solids," CRC Press, New York, 1999.
14. Zener, C.: "Elasticity and Anelasticity," University of Chicago Press, Chicago, Ill., 1948.
15. Wert, C.: "The Metallurgical Use of Anelasticity" in "Modern Research Techniques in Physical Metallurgy," American Society for Metals, Cleveland, Ohio, 1953.
16. Jones, D. I. G.: *J. Sound and Vib.*, **140**:85 (1990).
17. Fay, J. J., et al.: *Proc. ACS Div. Polymetric Mat'ls. Sci. and Eng'g.*, **60**:649 (1989).
18. Fujimoto, J., et al.: *J. Reinf. Plastics and Composites*, **12**:738 (1993).
19. Chang, M. C. O., et al.: *Proc. ACS Div. Polymetric Materials Sci. and Engg.*, **55**:350 (1986).
20. Weibo, H., and Z. Fengchan: *J. Appl. Polymer Sci.*, **50**:277 (1993).
21. Cochardt, A.: *Scientific Paper* 8-0161-P7, Westinghouse Research Labs., W. Pittsburgh, Pa., 1956.
22. Person, N., and B. J. Lazan: *Proc. ASTM*, **56**:1399 (1956).
23. Torvik, P.: Appendix 72fg, *Status Rep.* 58-4 by B. J. Lazan, University of Minnesota, Wright Air Development Center, Dayton, Ohio, Contract AF-33(616)-2802, December 1958.
24. Whittier, J. S., and B. J. Lazan: Appendix B, *Prog. Rep.* 57-6, Wright Air Development Center, Dayton, Ohio, Contract AF-33(616)-2803, December 1957.
25. Hinai, M., et al.: *Trans. Japan. Inst. Met.*, **28**:154 (1987).
26. De Batist, R.: *ASTM Spec. Tech. Pub.* 1169, 45-59, American Society for Testing and Materials, Philadelphia, 1992.
27. Zhang, J., et al.: *Acta Met. et Mat.*, **42**:395 (1994).
28. Goodman, L. E., and J. H. Klumpp: *J. Appl. Mechanics*, **23**:241 (1956).
29. Lazan, B. J., and L. E. Goodman: "Shock and Vibration Instrumentation," p. 55, ASME, New York, 1956.
30. Pian, T. H. H., and F. C. Hallowell: *Proc. First U.S. Nat'l. Cong. Appl. Mechanics*, June 1951, p. 97.
31. Fluegge, W.: "Viscoelasticity," Blaisdell Publishing Company, a division of Ginn and Company, Waltham, Mass., 1967; Lee, E. H.: "Viscoelasticity," in W. Fluegge (ed.), "Handbook of Engineering Mechanics," McGraw-Hill Book Company, New York, 1962; Lesieutre, G. A.: *Int'l. J. Solids and Structures*, **29**:1567 (1992).
32. Bogdanoff, J. L.: *J. Appl. Physics*, **21**:1258 (1950).
33. Caughey, T. K.: *J. Appl. Mechanics*, **27**:640 (1960).
34. Rang, E.: *Wright Air Development Center Tech. Rep.* 59-121, February 1959.
35. Goodman, L. E.: "A Review of Progress in Analysis of Interfacial Slip Damping," in "Structural Damping," ASME, New York, 1959.
36. Deresiewicz, H.: "Bodies in Contact with Applications to Granular Media," in G. Herrmann (ed.), "R. D. Mindlin and Applied Mechanics," Pergamon Press, New York, 1974.